EFFECTS OF A ROTATING AERODYNAMIC PROBE ON THE FLOW FIELD OF A COMPRESSOR ROTOR

Jan Lepicovsky
ASRC Aerospace Corporation
NASA Glenn Research Center
Cleveland, Ohio, U.S.A.

ABSTRACT

An investigation of distortions of the rotor exit flow field caused by an aerodynamic probe mounted in the rotor is described in this paper. A rotor total pressure Kiel probe, mounted on the rotor hub and extending up to the mid-span radius of a rotor blade channel, generates a wake that forms additional flow blockage. Three types of high-response aerodynamic probes were used to investigate the distorted flow field behind the rotor. These probes were: a split-fiber thermo-anemometric probe to measure velocity and flow direction, a total pressure probe, and a disk probe for in-flow static pressure measurement. The signals acquired from these high-response probes were reduced using an ensemble averaging method based on a once per rotor revolution signal. The rotor ensemble averages were combined to construct contour plots for each rotor channel of the rotor tested. In order to quantify the rotor probe effects, the contour plots for each individual rotor blade passage were averaged into a single value. The distribution of these average values along the rotor circumference is a measure of changes in the rotor exit flow field due to the presence of a probe in the rotor. These distributions were generated for axial flow velocity and for static pressure.

NOMENCLATURE

Symbols

C_{SP}	[*1*]	static pressure coefficient $\{(p_{SP} - P_{AMB})/(0.5*\rho*U_{BT}^2)\}$
C_{TP}	[*1*]	total pressure coefficient $\{(p_{TP} - P_{AMB})/(0.5*\rho*U_{BT}^2)\}$
C_{VX}	[*1*]	axial velocity coefficient $\{V_{VX}/U_{BT}\}$
h	[*mm*]	radial coordinate
n	[*%*]	relative rotative speed
p_{AMB}	[*kPa*]	ambient pressure
p_{SP}	[*kPa*]	static pressure
p_{TP}	[*kPa*]	total pressure
U_{BT}	[*m/s*]	rotor blade tip speed
V_{VX}	[*m/s*]	axial velocity component
V_{IN}	[*m/s*]	inlet average velocity
z	[*mm*]	rotor blade height
φ	[*1*]	compressor flow coefficient $\{V_{IN}/U_{BT}\}$
ρ	[kg/m^3]	air density
τ	[*1*]	rotor blade passage relative period
Θ_{VX}	[*%*]	fraction of rotor sector average (axial velocity component)
Θ_{SP}	[*%*]	fraction of rotor sector average (static pressure)

Abreviations

BR	blade root
BT	blade tip
CA	channel average
IGV	inlet guide vanes
LE	leading edge
LS	lower span
MS	mid span
OPR	once-per-revolution mark
PRB	rotor probe
RB	rotor blade
RBC	rotor blade channel
RBR1	stage 1 rotor blade row
S---	fixed measurement station (port)
SP	split plane of compressor shroud
SVR1	stage 1 stator vane row
US	upper span

MOTIVATION

In order to measure flow parameters in the relative flow frame of a spinning rotor directly, aerodynamic probes must be mounted in the rotor cascade. Placing probes in rotor blade channels, however, causes flow blockage, which affects the flow pattern in the follow-up stages of the machine under test. The work presented in this paper focused on an investigation of the effects of the rotating aerodynamic probe on the rotor outflow. A Kiel total pressure probe was mounted on the rotor hub at a mid-chord location in the first stage of the NASA Low Speed Axial Compressor (LSAC) to measure rotor inlet pressure in the relative flow frame. The probe extended up to the mid-span radius of the rotor. The probe generates a wake that forms an additional flow blockage in the given rotor channel. It is intuitively obvious that the flow field in this particular blade channel will differ from the flow field patterns in the remaining rotor channels. It is not quite clear, however, what are the probe wake effects and how much this probe wake will modify the flow field at the inlet plane of the adjacent stator cascade. Also, it is not clear if the wake effects are contained to the particular rotor blade channel only, or by how much the flow field in the neighboring rotor channels is also affected.

LOW SPEED AXIAL COMPRESSOR

The NASA LSAC test facility was utilized for this study. The LSAC facility is described in detail in Refs. 1 through 3, so only the basic characteristics are stated here. The research compressor comprises an inlet guide vane row followed by four geometrically identical axial stages (rotors and stators). The case radius is *610 mm*, and the hub radius is *488 mm*; thus the hub/tip ratio is *0.8*. The rotor has *39* blades. The rotor blade channel throat area is *5320* mm^2. Compressor design flow coefficient is *0.395*. The compressor was operated during this entire investigation at a constant physical speed of *984 ± 1 rpm* ($n = 100\%$) at the last stable operation point close to the surge limit ($\varphi = 0.345$).

The Kiel probe, mounted in the first stage rotor, is shown in the photographs of Fig. 1. The location of the rotor probe with respect to the once-per-revolution (*OPR*) mark is shown in Fig. 2. The *OPR* mark, a black stripe, is used in conjunction with an optical pickup to generate a single voltage pulse per each rotor revolution. As seen in Fig. 2, the rotor blades are labeled for identification. The Kiel probe is located in rotor blade channel *RBC29*, which is between rotor blades *RB29* and *RB30*. The probe extends to the channel mid-span radius, where the probe occupies a projected area of *185* mm^2. It follows that the geometric blockage due to the probe presence in the blade channel is *3.5%*. The two aluminum blades *RB33* and *RB34* had no particular meaning for this investigation.

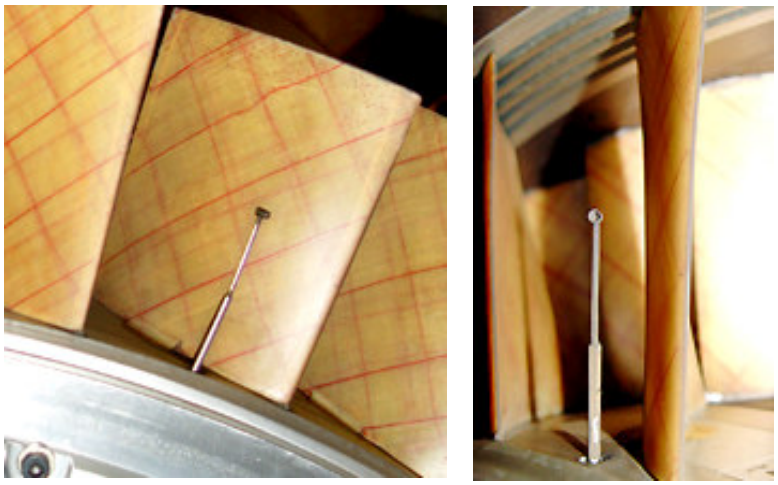

Fig. 1. The total pressure probe in a rotor blade passage.

The compressor partial layout is shown in Fig. 3. The axial section, depicted in the upper right quadrant, covers only the inlet guide vane row, and both rows of the first stage. In the compressor cross-section, only part of the compressor left half is shown. The position of the rotating probe in the rotor leading edge plane, as well as the fixed measurement stations behind the first stage rotor are clearly identified in the drawings. All dimensions are related to the split plane of the compressor shroud. The angular positions of the fixed measurement stations are related to the "12 o'clock" point on the compressor shroud. The optical pickup for the *OPR* signal is at the

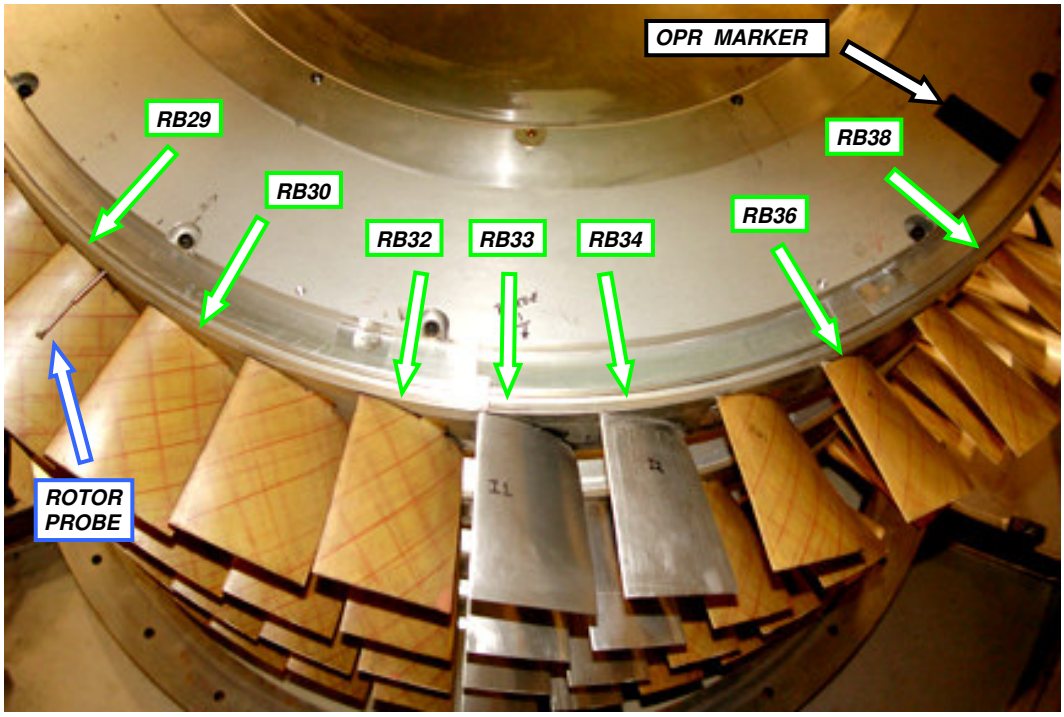

Fig. 2. View of the first rotor (*OPR* = once per revolution, *RB* = rotor blade).

"6 o'clock" position. Blading of the compressor first stage and a layout of measurement stations are presented in Fig. 4. The rotor probe (*PRB*) is, of course, moving with the rotor. The stations *S15A* and *S15B* are probe ports made in the compressor shroud, and therefore they are at fixed positions. High-response aerodynamic probes to determine changes in the rotor flow field due to the *PRB* wake were inserted into the compressor through these ports.

INSTRUMENTATION

Three types of high-response aerodynamic probes were used to investigate the unsteady flow field behind the rotor. These probes were: a split-fiber thermo-anemometric probe to measure velocity and flow direction, a total pressure probe, and a disk probe for in-flow static pressure measurement. The probes are shown in Figs. 5, 6, and 7; detailed descriptions of these probes are in Refs. 3 and 4, so only the basic data are given here. The frequency response of the commercial (Dantec Inc.) split-fiber probe used is flat up to at least *10 kHz* (Ref. 3), which is sufficient for reliable unsteady velocity acquisition in the LSAC facility (blade passing frequency is only *640 Hz*). Details of the signal decomposition procedure for the split-fiber probe to distinguish between velocity and flow direction signals are given in Ref. 3. Both pressure probes, total and static, are in-house designs, and are described in detail in Ref. 4. The probes have built in miniature Kulite pressure transducer with a *7 kPa* (*1 psid*) pressure range. The total pressure probe has a flat frequency response up to *35 kHz*, whereas the disk static pressure probe frequency limit is *70 kHz*.

The high-response aerodynamic probes were inserted one after another in the gap behind the rotor through the same access ports (*S15A* and *S15B*), and the compressor was repeatedly operated at the same conditions. The probes were traversed along the rotor blade span starting at the compressor shroud to acquire data over the entire rotor flow field.

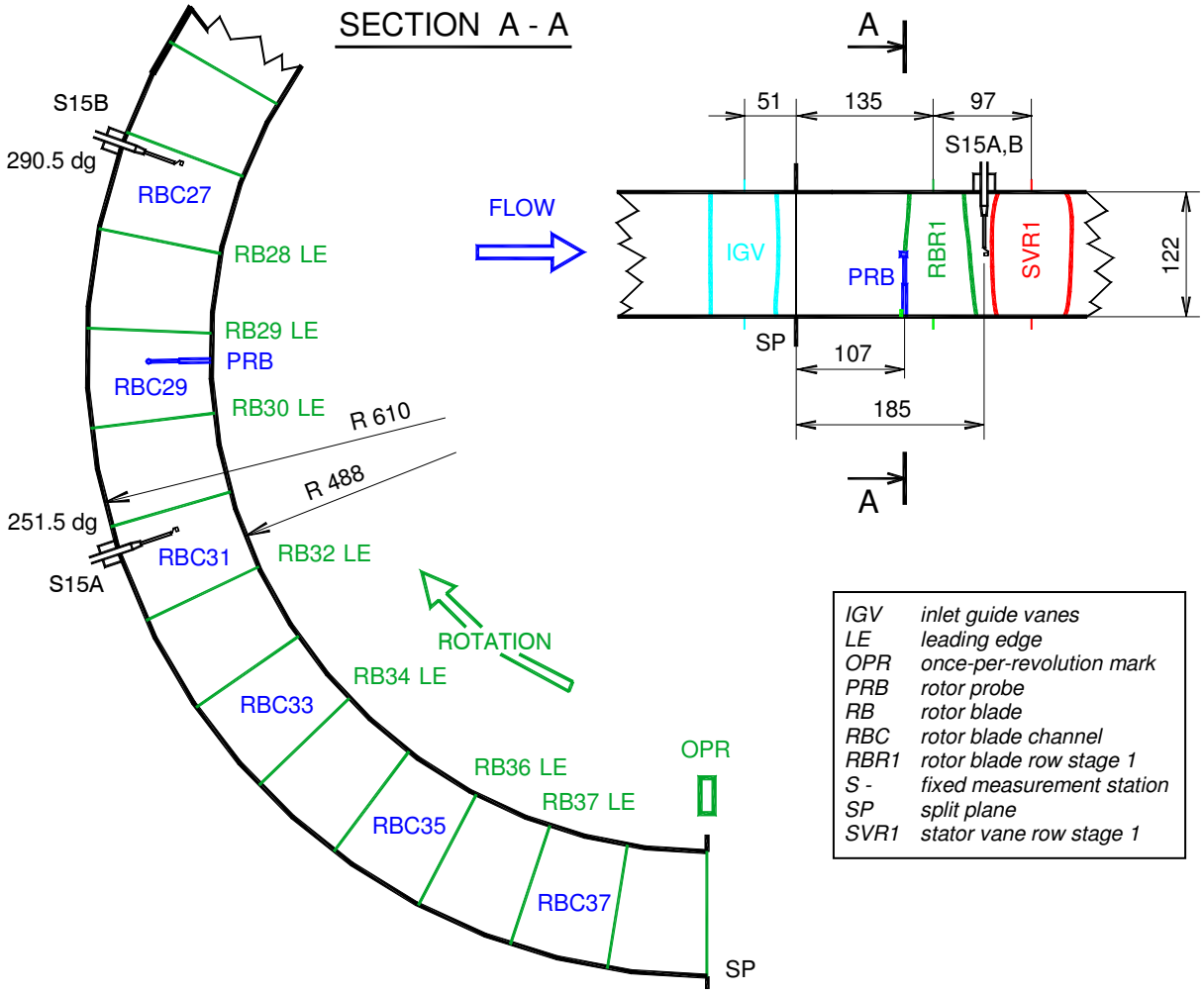

Fig. 3. Layout of measurement stations and compressor basic dimensions.

ROTOR ENSEMBLE AVERAGING

The signals acquired from high-response probes were reduced using an ensemble averaging method based on a once per rotor revolution signal. Using this method, continuous data records five seconds long were subdivided into *65* segments, each segment being equal to one rotor revolution, and all segments were averaged into a resulting distribution equal to the rotor revolution period. Parsing the resulting distribution into *39* subsegments (the rotor investigated has *39* blades) separate distributions for each rotor blade channel were acquired. This procedure was applied to every span position of the probes that were traversed behind the rotor. In this way, individual contour plots for each rotor channel were constructed.

CONTOURS OF FLOW PARAMETERS

In order to show clearly the effects of the rotor probe on the flow field in the rotor passages involved, only parts of the entire rotor flow field will be shown. As seen in Figs. 2 and 4, the rotor blade channel most affected is channel *RBC29*. Because the majority of rotor blade channels is not affected by the probe presence, only two of three channel groups will be shown. The first group, the wake channels group, comprises channels *RBC28*, *RBC29*, and *RBC30*, and the second group, the free flow group, which is *180 dg* from the wake group, comprises channels *RBC10*, *RBC11*, and *RBC12*. As a rule, the free flow group is always shown first in the following contour plots.

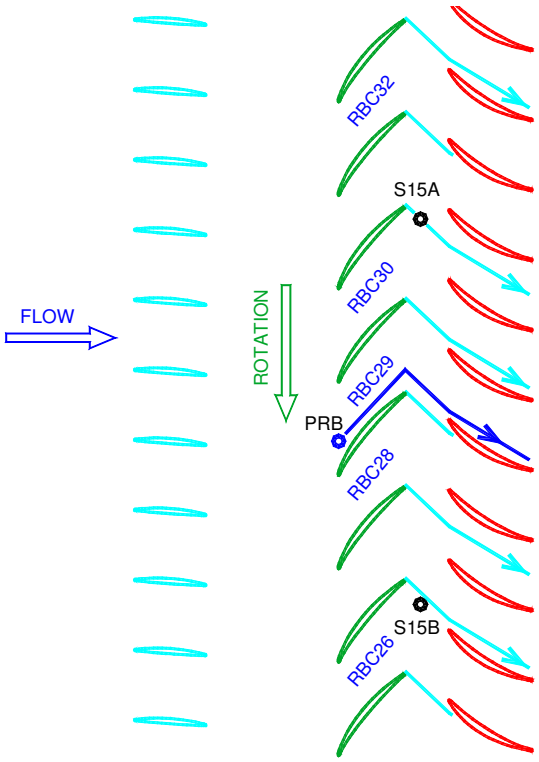

Fig. 4. First stage blading and projected wake trajectory of the rotor probe.

As indicated in Figs. 3 and 4, there are two access ports in the compressor shroud *S15A* and *S15B*. Inspecting Fig. 4, it can be seen that the port *S15A* is located close to a flow stream line that enters the stator cascade at the mid-pitch of the stator vane channel. On the other hand, the port *S15B* is on a flow stream line heading for the stator vane stagnation region. Consequently, the differences between flow parameter contours generated for these two ports must reflect the effects of stator vanes on the rotor flow field.

Contours of axial velocity coefficient for the free flow channels for both access ports are presented in Fig. 8. As seen here, there are no visible differences in the flow patterns of individual channels for a given port. As discussed above, the velocity levels are lower for the *S15B* port (stator vane stagnation region) than for the *S15A* port (mid-pitch region of the stator vane channel). The situation is quite different for the wake channels group (Fig. 9). As expected, the flow pattern in channel *RBC29* is severely affected by the rotor probe wake. Flow is heavily blocked and separated from the suction surface in this channel (the affected area is over *20%* of the entire blade channel). The suction surface of the next channel (*RBC30*) also suffers larger separation than it was for the free flow channel, albeit significantly smaller than that for channel *RBC29*.

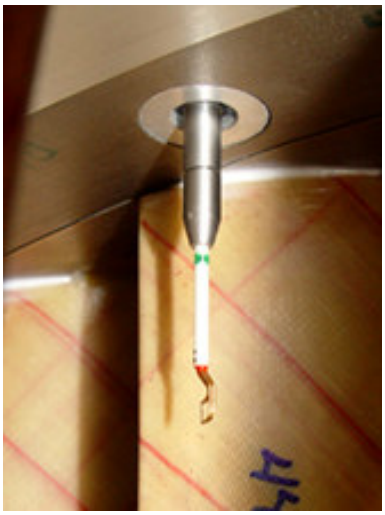

Fig. 5 Split-fiber probe in the gap between rotor and stator of the compressor first stage.

Fig. 6 Unsteady total pressure probe installed in an axial research compressor.

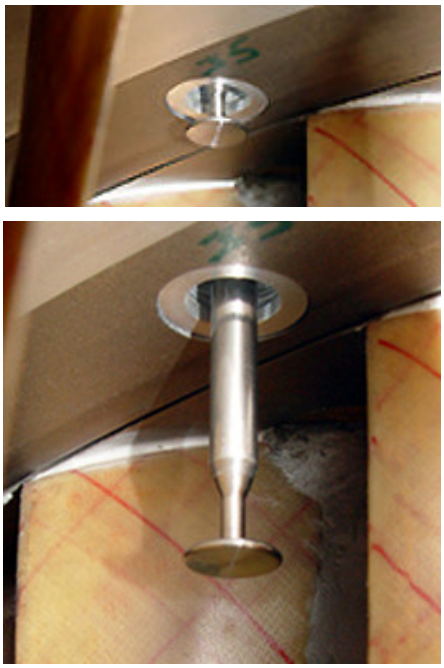

Fig. 7 Disk probe for in-flow unsteady static pressure measurements (shown at two span positions).

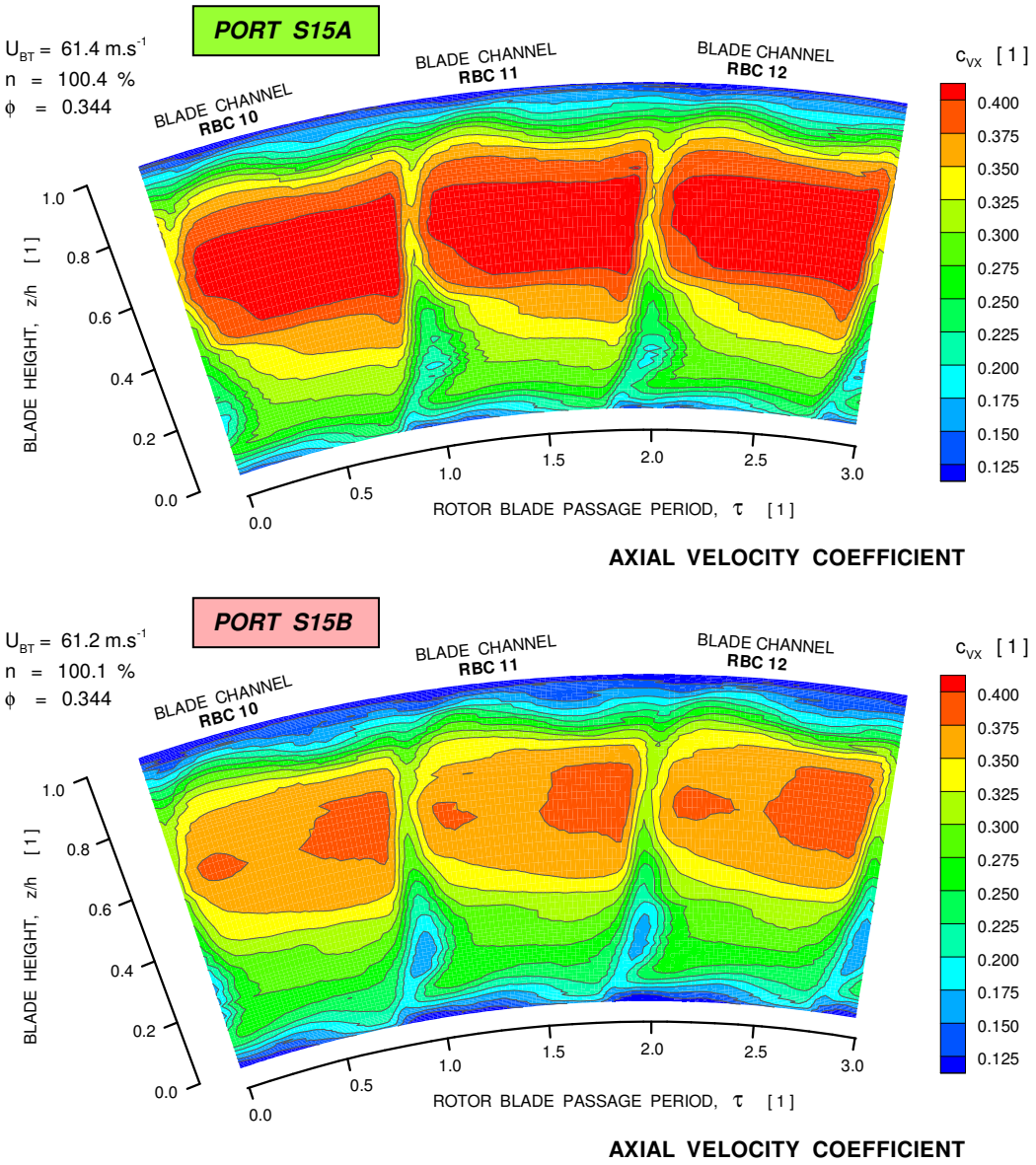

Fig. 8. Contours of axial velocity coefficient for the free flow channels group.

Static pressure coefficient data are presented in Figs. 10 and 11. Static pressure patterns for the free flow cannels measured at port *S15A* are noticeably different from those measured at port *S15B* (Fig. 10). In general, the static pressure in both data sets increases toward the blade tip. However, for station *S15A* (mid pitch of stator vane channel) the pressure levels are quite low, and in particular in the rotor blade wake regions the static pressure depressions extend up to *70%* of the blade span. For station *S15B* (stator vane stagnation region) zones of high pressure spread from the blade tip down to *20%* of the blade span. Static pressure patterns for the wake channels group (Fig. 11) are, at first glance, somewhat similar to the free flow channels group. For station *S15A* (mid pitch) the difference from the free flow channels is mostly in channel *RBC29*, where an extended zone of low pressure close to the rotor hub can be observed. At station *S15B* (vane stagnation region), the difference can be observed mainly along the pressure surface of channel *RBC28*.

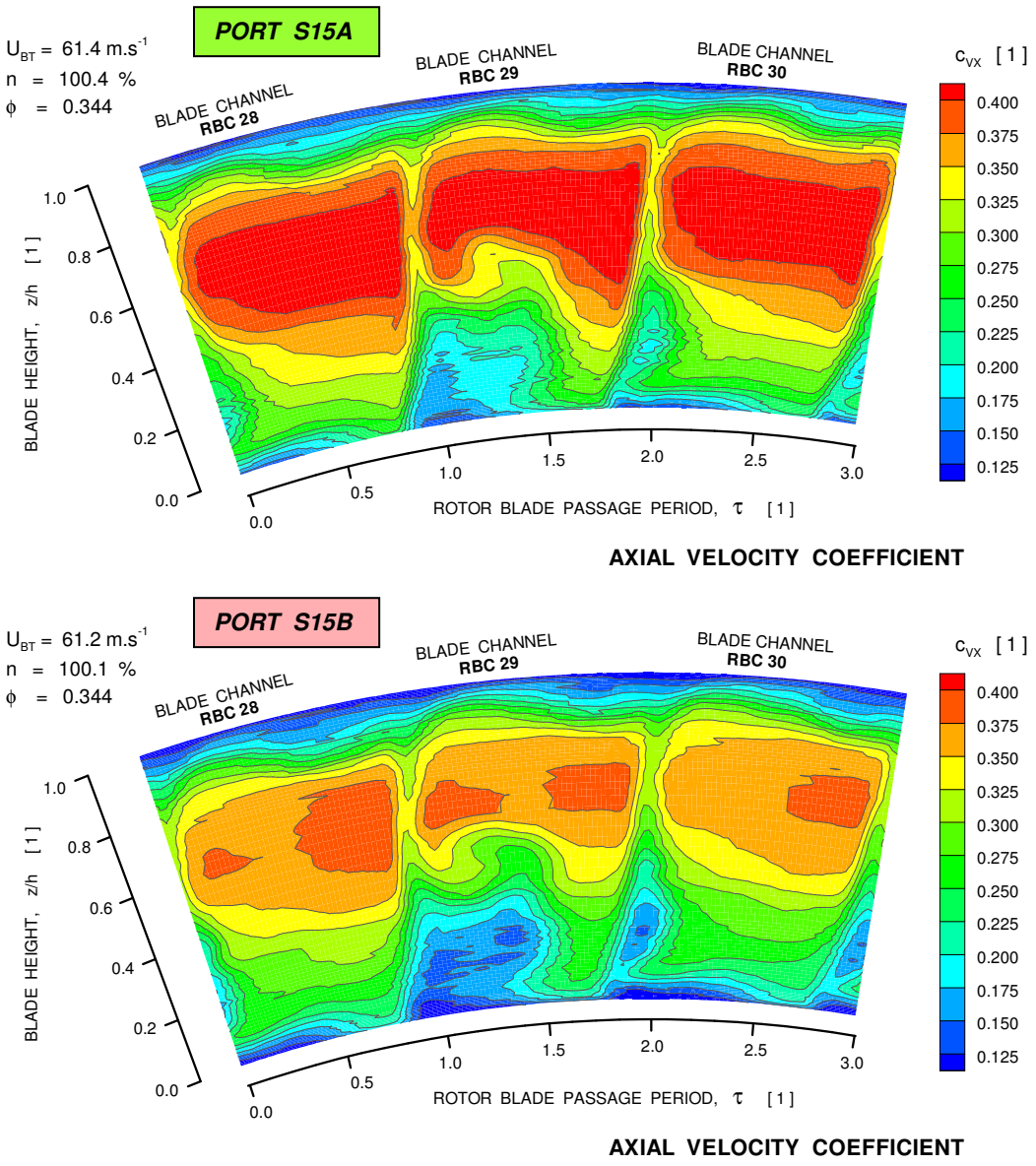

Fig. 9. Contours of axial velocity coefficient for the wake channels group.

Finally, contours of total pressure coefficient are introduced in Figs. 12 and 13. Total pressure contours for the free flow channels appear quite uniform over the most of the rotor channel area. There are limited regions of higher pressure at mid pitch, just at the compressor shroud (blade tip). These spots are probably associated with the blade tip cross flow. Further, there are stripes of elevated pressure along the full span of the blade channel pressure surface, and finally, there are pressure depression zones at the blade channel suction surface close to the blade roots. The major difference between data for stations *S15A* and *S15B* is that the pressure pattern variations described seem to be more extreme for the stator mid-pitch data (*S15A*) than for the vane stagnation region (*S15B*). It is as if the stagnation regions of the stator vanes smoothed out the total pressure variations. The situation for the wake channels group differs from the previous one mainly by enlarged total pressure depression in the hub and the suction surface corner of blade channel *RBC28*, noticeable pressure increase in the hub region of blade channel *RBC 29*, in particular in the hub and pressure surface corner of this

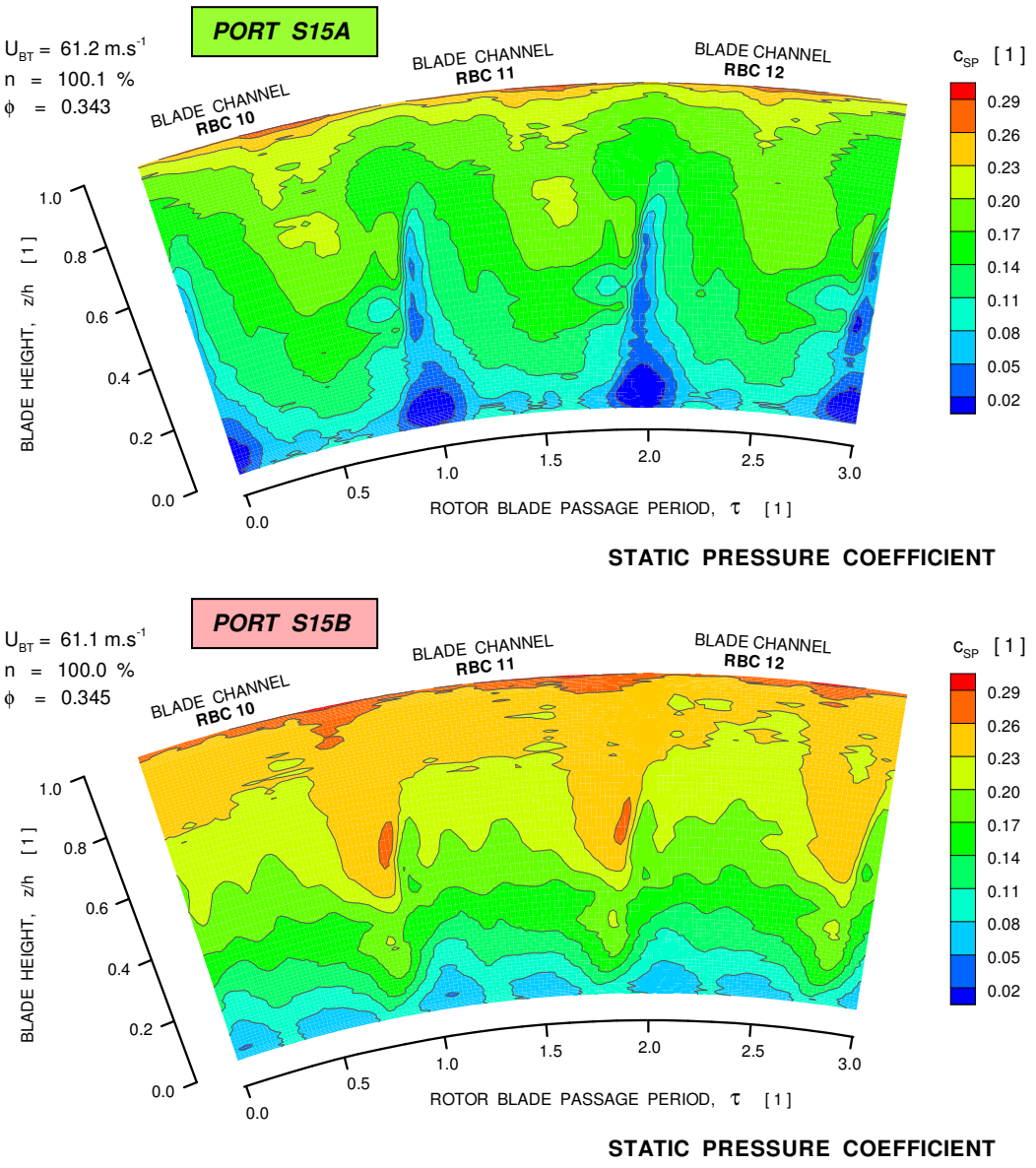

Fig. 10. Contours of static pressure coefficient for the free flow channels group.

blade channel. The zone of increased total pressure in the hub region of channel *RBC29* is probably a manifestation of increasing tangential velocity component in this region on the account of diminishing axial velocity (Fig. 9). There is no significant difference between vane mid-pitch data (*S15A*) and the vane stagnation region data (*S15B*).

CIRCUMFERENTIAL VARIATION OF CHANNEL AVERAGES

In order to quantify the rotor probe effects, the contour plots for each individual rotor blade passage were averaged into a single value. The distribution of these average values along the rotor circumference is a measure of changes in the rotor exit flow field due to the presence of a probe in the rotor. These distributions were generated for axial flow velocity and for static pressure.

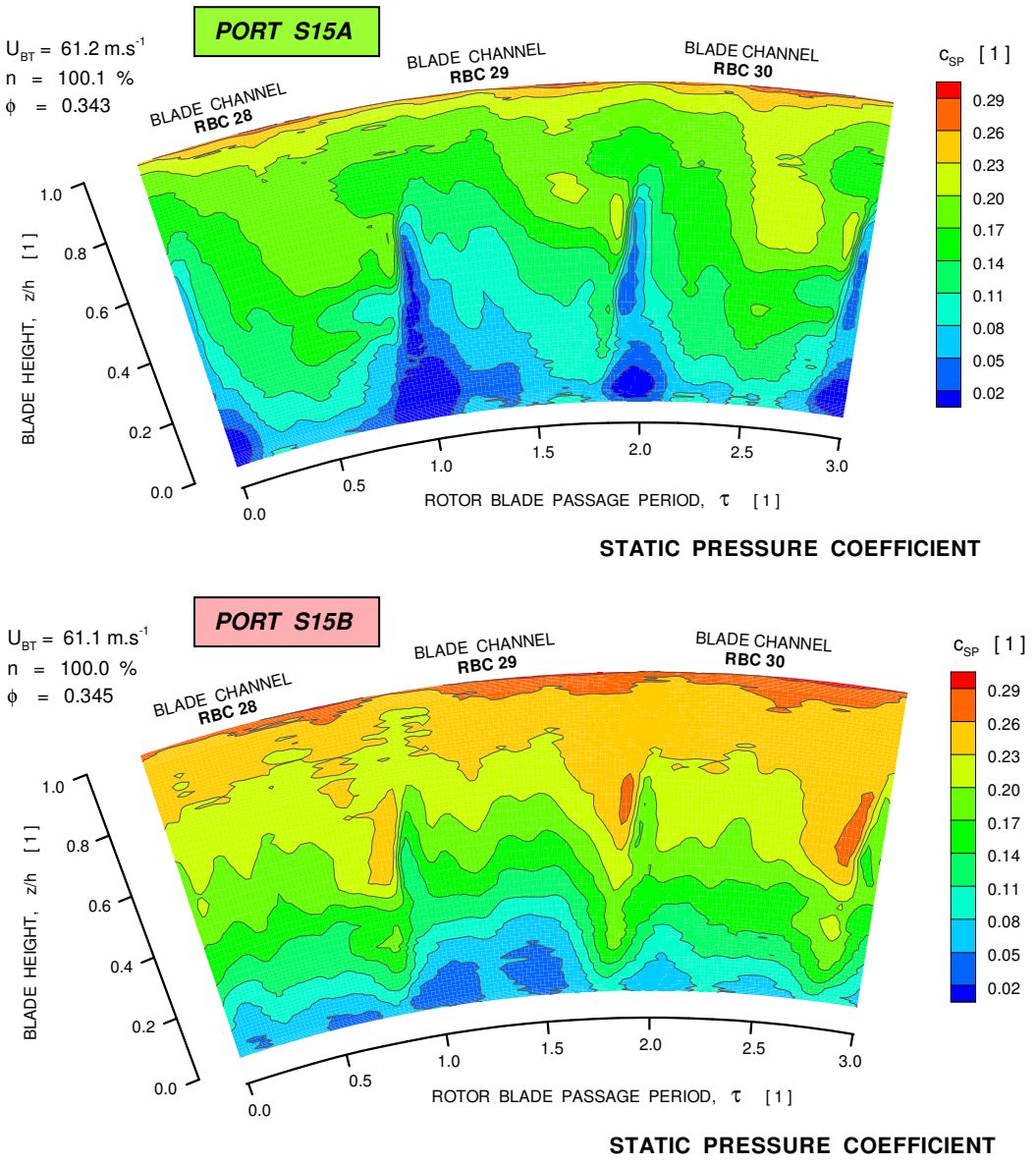

Fig. 11. Contours of static pressure coefficient for the wake channels group.

Several averages were calculated as is schematically indicated in Fig. 14. The first was the average over the entire area of a rotor blade channel. Then, sector averages, which are averages for partial channel area, were calculated. These averages are called: (1) blade tip sector (calculated over an area between *80%* and *100%* of the blade span), (2) upper span sector (area between *60%* and *80%* of the blade span), (3) mid span sector (area between *40%* and *60%* of the blade span), (4) lower span sector (area between *20%* and *40%* of the blade span), and finally (5) blade root sector (area between *0%* and *20%* of the blade span).

Circumferential variations of rotor channel average axial velocity are presented in Fig. 15. The top most bar diagram in this figure presents the distribution of channel overall averages. The abscissa identifies all *39* rotor blade channels, and the ordinate records axial velocity coefficient. As seen in this diagram, the average value for most of the channels in nearly identical except for channel *RBC29*, that shows a noticeable depression.

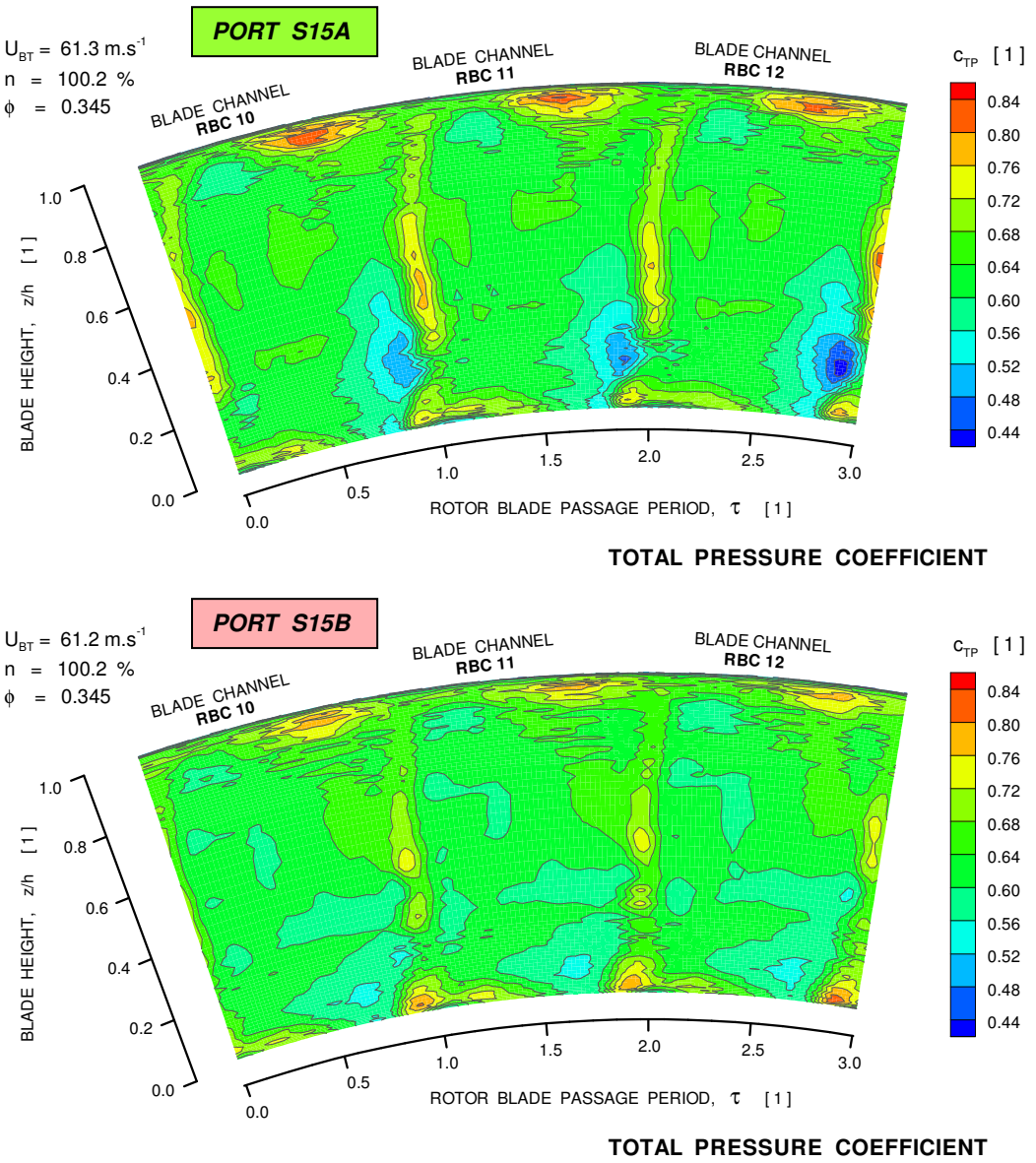

Fig. 12. Contours of total pressure coefficient for the free flow channels group.

This is the channel which contains the rotor probe. It appears that the neighboring channels *RBC28* and *RBC30* show a slight increase in the axial velocity, probably counterbalancing the velocity deficit in channel *RBC29*.

An extremely interesting diagram is the next diagram for the blade tip sector that reveals huge variations of axial velocity average values along the rotor perimeter. The reason for such huge variation is not obvious. It should be emphasized here that the diagram is an average over *65* rotor revolutions, so the variations are not random but highly repeatable. The upper span sector (the third diagram) indicates uniform averages for nearly all of the channels, again with an exception for channel *RBC29*. Contrary to the overall averages (the first diagram), channel *RBC29* has a visibly higher value than the rest of the channels. As seen in Figs. 1 and 2, the rotor probe blocks the lower half of the rotor channel *RBC29*. Obviously, the blockage in the lower half causes axial velocity increase in the upper half of the blade channel *RBC29*. The following three diagrams for mid span,

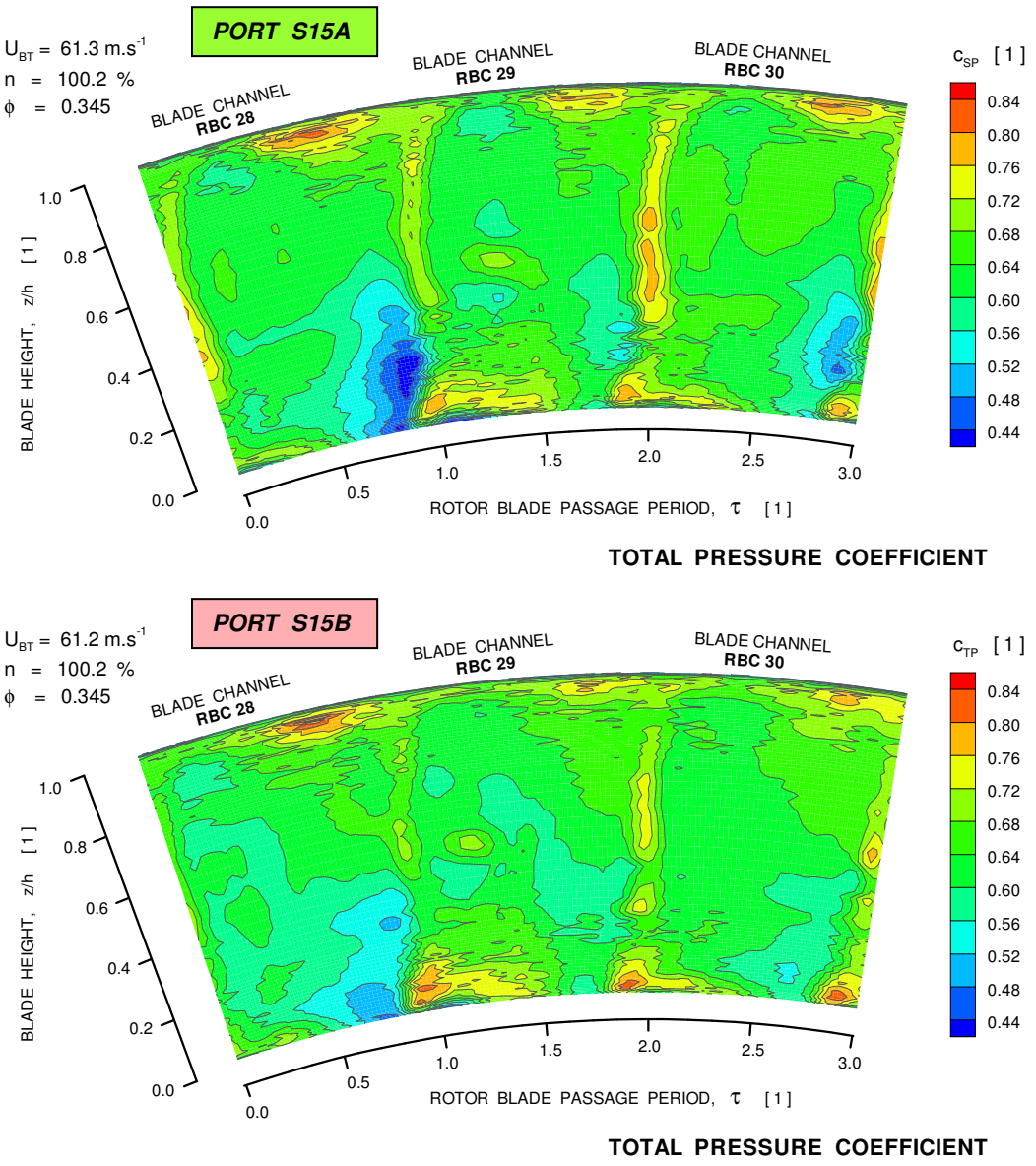

Fig. 13. Contours of total pressure coefficient for the free flow channels group.

Lower span, and blade root sectors show various degrees of a large axial velocity deficit for channel *RBC29*. In addition, they also show small but visible variations of axial velocity among the rest of the rotor channels.

The circumferential variations of channel averages for the static pressure coefficient indicate a different character than the axial velocity coefficient, as is immediately obvious in Fig. 16. First, all the diagrams in this figure show the same character, varying only in a degree of pressure depression for channel *RBC29*. Contrary to the axial velocity diagrams, the probe effect is not limited to channel *RBC29* only, but a pressure depression is clearly visible also in channel *RBC28,* which precedes the rotor channel containing the probe.

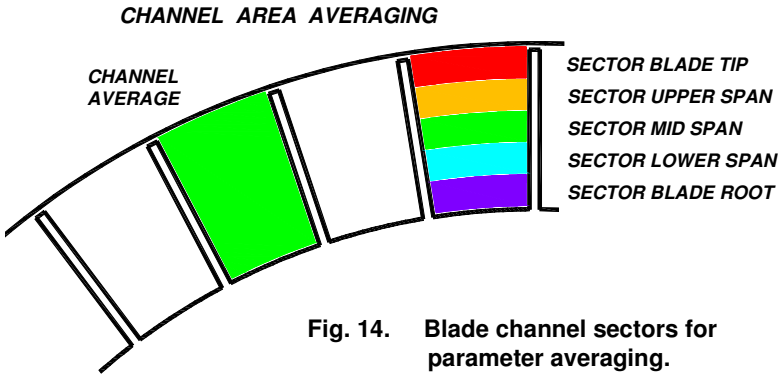

Fig. 14. Blade channel sectors for parameter averaging.

CONCLUSION

Mounting a probe in the rotor causes deterioration in the rotor outlet flow. The defects in static pressure and axial velocity component due to the presence of an aerodynamic probe in the rotor are summarized in Fig. 17. The diagram on the left hand side is for static pressure coefficient, and that on the right hand side is for axial velocity coefficient. The abscissa in both diagrams identifies blade channel average (*CA*), and the following sectors: blade tip (*BT*), upper span (*US*), mid span (*MS*), lower span (*LS*), and blade root (*BR*). The ordinate records the flow parameter depression in an affected rotor blade channel as a fraction of the parameter average taken over all remaining channels not affected by the rotor probe presence. It was shown in Figs. 15 and 16 that in the case of axial velocity only channel *RBC29* was affected by the probe wake, whereas for static pressure case two channels *RBC28* and *RBC29* were affected. Therefore, only these two channels are shown in Fig. 17.

As seen in Fig. 17 the probe presence is manifested for the channel overall average as well as for all the sector averages. For the static pressure coefficient, the value in channel *RBC28* is about *95%* of the average value, and for channel *RBC29* it is only *86%*. Both channels show static pressure depression along the entire blade span. The effects on the axial velocity coefficient are shown in the diagram on the right hand side of Fig. 17. The axial velocity level in channel *RBC29* is lower than is the average of the rest of the rotor channels (down to *96%*); however, for the sector averages the situation is different. In the upper half of the blade channel, *RBC29* (sectors *BT* and *US*), the axial velocity is higher than the average level (about *103%*), and then rapidly drops down to about *88%* in the lower half of the rotor blade channel (sectors *MS*, *LS*, and *BR*). Clearly, the consequence of increased blockage and decreased axial velocity in the lower channel half is an increase in axial velocity component in the upper, unblocked, portion of the rotor blade channel.

The qualitative and quantitative findings about the flow field distortion due the presence of an aerodynamic probe in a compressor rotor do not tell the entire story. A probe mounted in a compressor rotor will undoubtedly also affect onset of rotating stall and stability limits of a compressor tested. Such investigations, however, were beyond the scope of this study.

ACKNOWLEDGEMENT

The work was sponsored by the NASA Glenn Research Center under the Intelligent Propulsion Systems Foundation Technologies by Dr. C.R. Mercer. The author would like to thank Mr. J.P. Veres, chief of the GRC Compressor Branch for his support and permission to publish the results of this study. Significant help from Mr. E.P. Braunscheidel of NASA GRC in managing the test facility operation is particularly acknowledged.

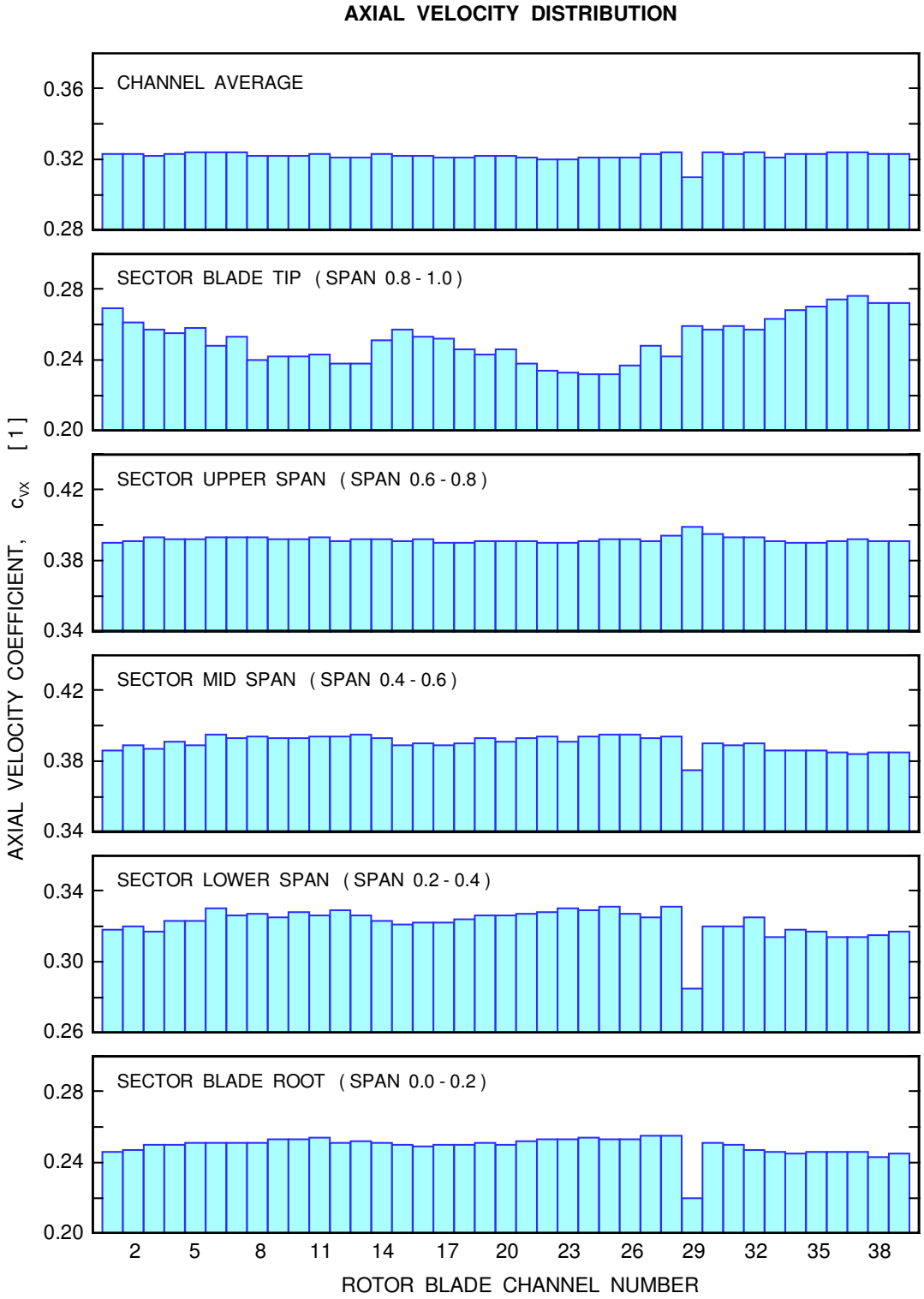

Fig. 15. Channel averages of axial velocity coefficients.

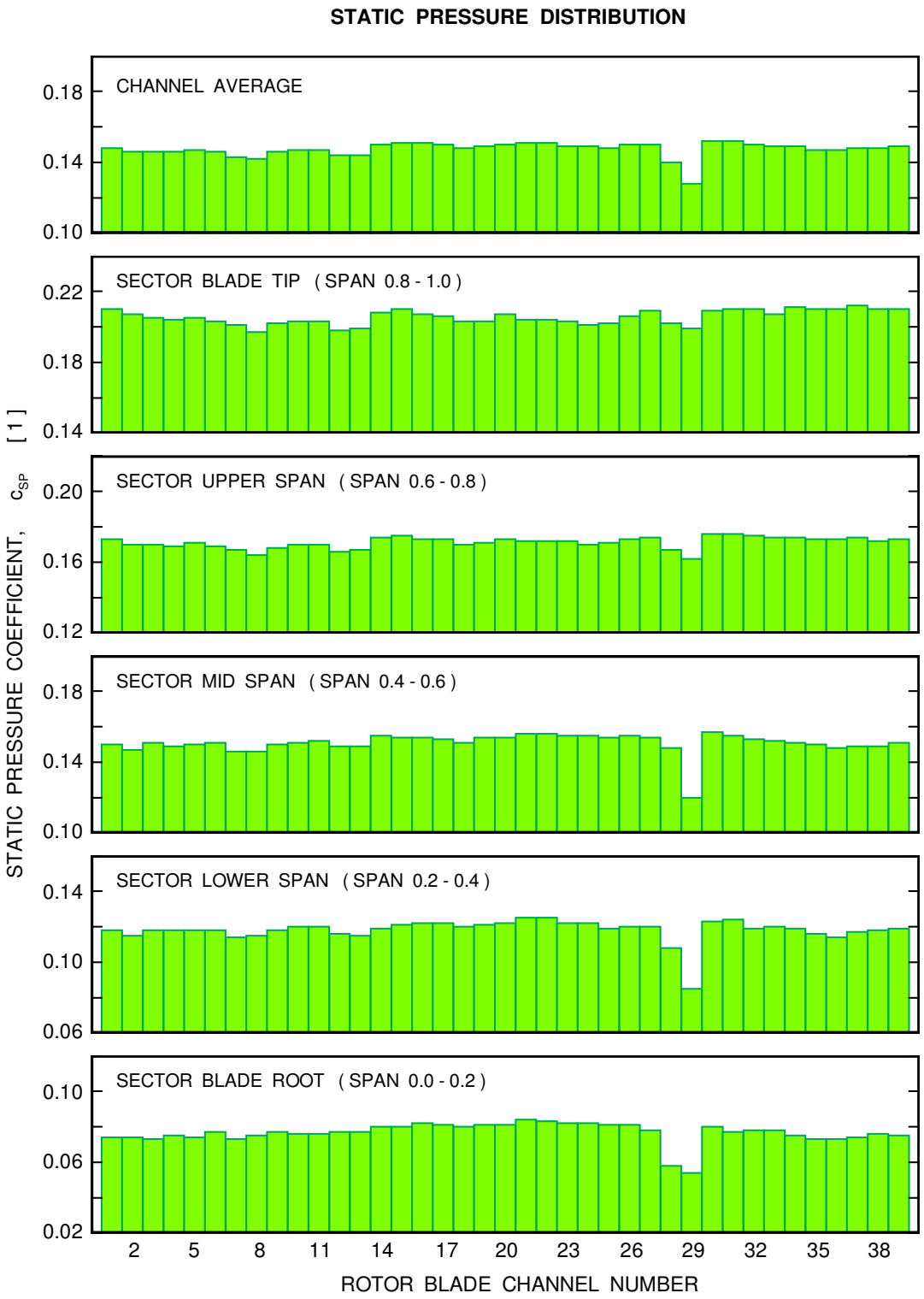

Fig. 16. Channel averages of static pressure coefficients.

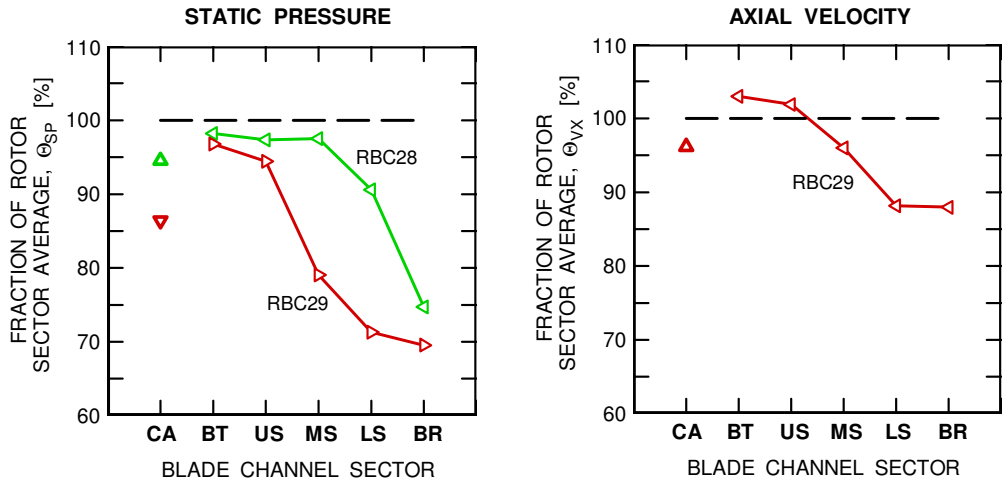

Fig. 17. Wake channel parameter level relative to sector average.

REFERENCES

1. Wasserbauer, C.A., Weaver, H.F., and Senyitko, R.G.: "NASA Low-Speed Axial Compressor for Fundamental Research", NASA TM-4653, 1995.
2. Wellborn, S.R. and Okiishi, T.H.: "Effects of Shrouded Stator Cavity Flows on Multistage Axial Compressor Aerodynamic Performance", NASA CR-198536, 1996.
3. Lepicovsky, J.: "Unsteady Velocity Measurements in the NASA Research Low Speed Axial Compressor", NASA CR-214815, 2007.
4. Lepicovsky, J.: "Measurement of Flow Pattern within a Rotating Stall Cell in an Axial Compressor", ASME paper GT-2006-91209, NASA/TM-2006-214270, 2006.